Segmenting Abnormalities and Predicting Breast Cancer in Ultrasound Images using Modified UNET Architecture

Ganesh Paudel

Nepal College of Information Technology,
Pokhara University
paudelganesh10@gmail.com

Niranjan Khakurel

Nepal College of Information Technology,
Pokhara University
niranjan@ncit.edu.np

Abstract— **Breast cancer is still a major worldwide health concern, and better patient outcomes and effective treatment depend on early identification. Different algorithms try to classify the breast cancer either malignant or benign or try to segment the abnormal section with the medical images. Convoluted Networks like Convolutional Neural Network (CNN) are broadly used for classification whereas U-shaped network like UNet, DeepLab are used for segmentation. This study suggests a multi-tasking UNet architecture where a single model perform both the classification and segmentation task over breast cancer BUSI dataset. Two different nature of dataset a) grayscale USG image with labels and b) grayscale with ground truth mask is sent as input. The model is trained under the train test split ratio of 80:10:10. In classification, the model achieved 98.36□0.62% of Training accuracy, 98.30 ± 0.94 % of Validation accuracy and 98.08 ± 0.64% of Testing Accuracy along with 0.19 ± 0.31, 0.092 ± 0.13 and 0.122 ± 0.18 Training loss, Validation loss and Testing loss respectively, whereas in Segmentation, the model achieved Intersection over Union (IoU) value of is 89.089%. The achieved results hold significant promise for advancing the field of medical image analysis, ultimately contributing to improved diagnosis and treatment outcomes for breast cancer patients.**

I. INTRODUCTION

Breast cancer develops when something goes wrong in the breast cells and is a serious health issue. Men are also susceptible to it though less frequently than women. It is the most common cancer among women accounting for nearly 25% of all diagnosed cancer cases and claiming hundreds of thousands of lives each year according to the World Health Organization (WHO) [1]. Early detection of breast cancer is crucial because it allows for better treatment options and increases the likelihood that patients will recover. As a result finding breast cancer early on is like a race against time.

Female breast cancer has now become the most commonly diagnosed cancer surpassing even lung cancer with an estimated 2.3 million new cases, accounting for 11.7% of all cancer diagnoses. However it's disheartening to note that breast cancer is also responsible for a significant number of fatalities with 6.9% of cancer-related deaths occurring in females due to breast cancer [2]. According to the statistics provided by Global Cancer Observatory (GLOBOCAN) for the year 2020 in Nepal, there were more new cases of cancer in women than in men. Specifically, there were 11,565 new cases in women and 8,943 in men. Among the different types of cancer that affect women, the top five most common ones were Cervix uteri, Breast, Lung, Gallbladder, and Ovary. Breast cancer was a significant concern ranking as the third

most common cancer in women in Nepal. In 2020, there were 1,973 new cases of breast cancer in women, making up 9.3% of all new cancer cases in females. Unfortunately, breast cancer also led to a significant number of deaths among women. It ranked as the fourth most deadly cancer for females in 2020. A total of 1,049 women lost their lives due to breast cancer accounting for 7.7% of all cancer-related deaths in women [3]. This highlights how serious breast cancer can be. It's essential to continue efforts to detect and treat it early to save lives.

Mammograms and biopsies are still commonly used by physicians and other healthcare professionals to detect and diagnose breast cancer. Mammograms are similar to specialized X-rays of the breasts and biopsies entail removing a small sample of breast tissue for analysis. Although these techniques have been extremely useful occasionally, they are flawed. They may mistakenly diagnose someone with cancer when they don't or they may fail to detect cancer when it is present. Therefore, it requires better and more precise methods for predicting and diagnosing breast cancer.

Artificial Intelligence (AI) is a type of super-smart computer technology. It can be trained to quickly and accurately understand and analyze medical information. AI is already assisting doctors by detecting problems in medical images such as X-rays and MRIs. In the case of breast cancer

AI can use its intelligence to improve detection and understanding.

Deep learning is a fancy term for computers that are extremely good at understanding images. U-Net models are more effective for segmenting breast cancer in ultrasound images because they are specifically designed to focus on the unique aspects of these images resulting in improved accuracy. Their specialized architecture allows them to identify subtle details critical for accurate diagnosis. Additionally, these models provide transparency by explaining their decision-making process which is valuable for medical professionals. They can adapt and improve with evolving medical knowledge reducing the risk of incorrect diagnoses. Ultimately U-Net model contribute to the early detection of breast cancer leading to better patient outcomes.

As a result, the focus of this study is on creating a residual U-Net model to assist doctors and healthcare professionals in better predicting and diagnosing breast cancer into two categories namely benign and malignant by analysing images. By doing so it easier to detect breast cancer early allowing people to receive appropriate treatment and remain healthy. By harnessing the power of AI and deep learning it is possible to make a significant difference in the fight against breast cancer and ultimately save lives.

Breast cancer is a critical global health issue, where early and accurate detection is compulsory for effective treatment and improved patient outcomes. Traditional approaches in medical image analysis employ distinct algorithms for either classification of breast cancer into malignant or benign categories or segmentation of abnormal regions within medical images. Convolutional Neural Networks (CNNs) are predominantly used for classification tasks, while U-shaped networks such as UNet and DeepLab are commonly employed for segmentation tasks [4] as shown in Figure 1. However, these methods typically require separate models for classification and segmentation, leading to increased computational complexity and inefficiency.
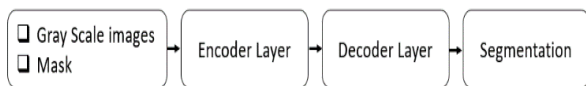

Fig. 1.   Workflow of Normal UNET Architecture

This study addresses the need for a more integrated and efficient approach by proposing a multi-tasking UNet architecture capable of performing both classification and segmentation simultaneously on the Breast Ultrasound Images Dataset (BUSI) dataset as shown in Figure 2.
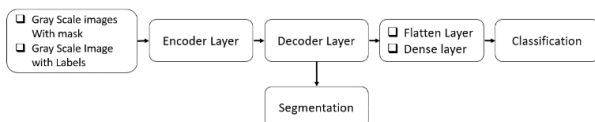

Fig. 2.   Workflow for Segmentation and Classification

The objectives of the study are – (1) To design the single U-Net Architecture to segment as well as classify the breast cancer dataset from Ultra Sound images; (2) To conduct a comprehensive performance evaluation and comparative analysis against established state-of-the-art methodologies.

II. Literature Review

A. U-Net

A neural network created especially for image segmentation is called the U-Net architecture [5]. Its basic structure consists of two different paths. The first is the contracting path, sometimes referred to as the encoder or analysis path. It offers classification information and has a look similar to a traditional convolutional network. The expanding path, also known as the decoder, is the second path; it combines features from the contracting path using up-convolutions and concatenations. This expansion path improves the output's resolution and allows the network to gather comprehensive localized categorization data. This improved resolution is then fed into a final convolutional layer to produce a fully segmented image as the final output. The U-shape of the entire network is almost symmetrical.
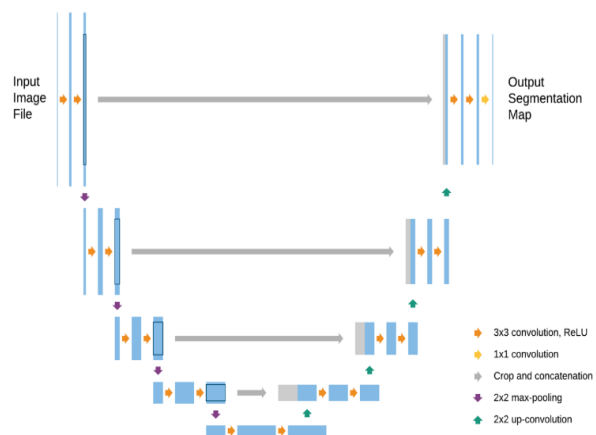

Fig. 3.   Basic U-Net Architecture

U-Net overcomes the drawbacks of traditional convolutional networks by offering pixel-level context, which is essential for medical image analysis where as traditional convolutional networks usually classify an entire image into a single label. While previous approaches tried to segment images, Ronneberger et al.'s U-Net model [5] represented a major breakthrough in medical image segmentation. This model was developed using fully convolutional networks, building upon the work of Long et al. [6]. As evidenced by its victory in the ISBI 2015 cell tracking challenge and its significant superiority over competing techniques, U-Net outperformed earlier techniques. The U-Net design is separated into two primary components, as was previously mentioned. The contracting path, which has a typical convolutional neural network (CNN) structure, is the first part. Two sequential 3x3 convolutions, a max-pooling layer, and an activation function known as the Rectified Linear Unit (ReLU) are the next steps in each block of this approach. There are several repetitions of this sequence.

The novel feature of U-Net is its wide trajectory. A 2x2 up-convolution is used to upsample the feature map at each step of this path. Next, the upsampled feature map is concatenated with the cropped feature map from the corresponding layer in the contracting path.

ReLU activation and two 3x3 convolutions come next in this process. To create the segmented output, the number of channels in the feature map is adjusted in the final stage using

a 1x1 convolution. Because pixel features at the borders have little contextual information and must be eliminated, cropping is crucial. By employing context from a wider, overlapping region, this architecture produces a U-shaped network that efficiently propagates contextual information throughout, enabling the segmentation of objects.

B. Convolutional Neural Network (CNN)

To extract the deep features and predict the results in more accurate way, Figure 4 shows the proposed skeleton of the CNN model. Convolutional Neural Networks (CNNs) are intended for picture recognition and processing. Their architecture is composed on numerous key layers. This is followed by activation layers such as ReLU, which introduce nonlinearity and enable the network to learn complex patterns. Pooling layers then lower the spatial dimensions of the feature maps using down sampling approaches such as max pooling, which control overfitting and reduce computations. The data passes through several convolutional, activation, and pooling layers before reaching fully connected layers, which combine the information to make final predictions. Finally, a softmax layer turns the outputs into classification probabilities.
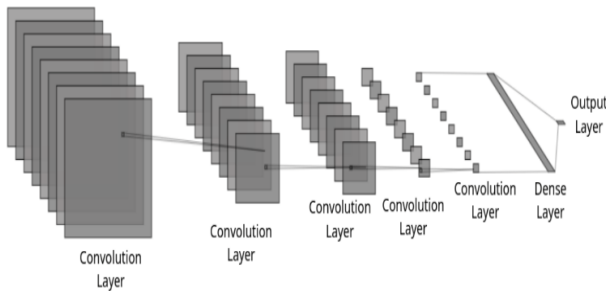

Fig. 4. Basic CNN Architecture

C. Breast Health Condition

1) Benign

The term "benign" refers to a non-cancerous condition or lump in the context of breast health. Consider the breast as a community of cells, similar to a quiet neighborhood. This cellular community may occasionally develop a small lump or bump. When healthcare professionals label it "benign," they are essentially com-paring it to having a friendly neighbor. In other words, there is no immediate dan-ger from this lump and it does not suggest cancer. CNNs are a type of deep neural network commonly used in computer vision applications. CNNs consist of multiple layers, including convolutional layers, pooling layers, and fully connected layers [7].

The majority of benign breast conditions are relatively stable and remain in their original location without any tendency to act aggressively. Since there is no risk of malignancy, healthcare professionals frequently decide to closely monitor these conditions to make sure they remain benign rather than rushing to pursue invasive treatments.
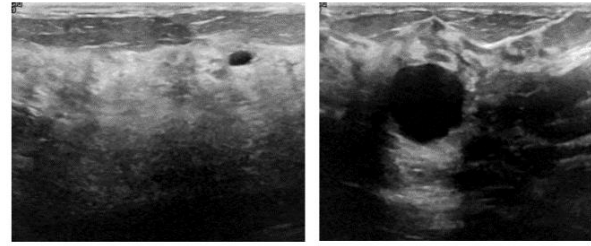

Fig. 5. Sample of Benign Image

2) Malignant

when it comes to breast health, the word "malignant" acts as a warning sign, de-noting the presence of a lump that could be cancerous. By labeling a lump as "malignant," medical professionals are essentially indicating that it is hostile and potentially dangerous [7]. Malignant breast conditions can be compared to disobedient children who break the rules. They spread uncontrollably and have the potential to spread to other parts of the body.

Healthcare providers must act quickly and decisively to treat malignant conditions. To halt the growth and progression of these problematic situations, they employ a variety of treatments, including surgery, medications, and radiation therapy. The goal is to prevent them from spreading and causing further harm, much like calling for help to deal with a dangerous intruder.
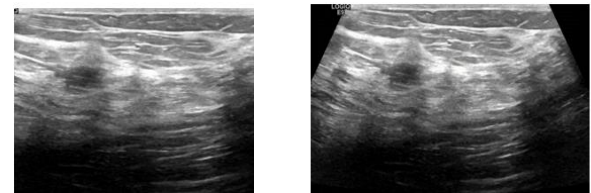
Fig. 6. Sample of Malignant Image

3) Normal

The term "normal" refers to situations or outcomes that do not show signs of ei-ther malignancy or benignity among the range of breast health assessments and findings. In essence, these are the observations and characteristics that fall within the range of expected and typical breast characteristics for the particular person. The absence of observable cancer symptoms, such as tumor formations or malig-nant growths, is shown by normal breast conditions. At the same time, they addi-tionally do not have any signs of benign alterations, such as non-cancerous cysts or fibroadenomas [7]. Fundamentally, normal breast conditions indicate that the breast tissue and its characteristics fall within the range of normal, healthy varia-tions, as anticipated for the person's age, gender and physiological characteristics.

Fig. 7.   Sample of Normal Image
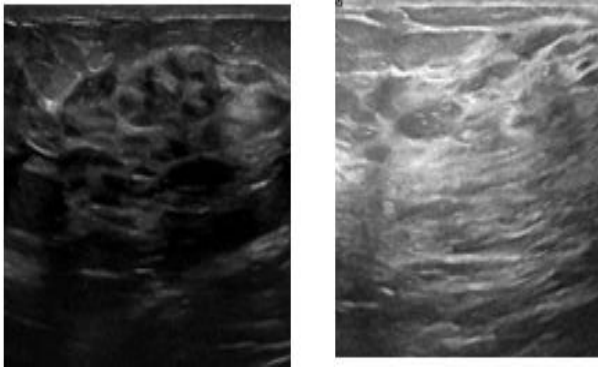
D. Related Work

The use of machine learning (ML), deep learning (DL), and transfer learning models can improve the capacity of computer-aided medical diagnosis for various breast health conditions, including benign, malignant, and normal, especially for ultrasound and CT images, according to a number of recent studies in medical image analysis.

In 2019, Khan et al. used transfer learning and deep learning algorithms to classify breast cancer images as benign or malignant [8]. They used pre-trained models like GoogLeNet, VGGNet, and ResNet to extract characteristics from photos. By applying average pooling, these features were then incorporated into fully connected layers. Their study utilized both a standard benchmark dataset and a locally developed da-taset, comprising a total of 8,000 images—6,000 for training the network and 2,000 for testing. The classification accuracies achieved were 93.5% with GoogLeNet, 94.15% with VGGNet, and 94.35% with ResNet. The custom CNN method they proposed achieved an impressive average accuracy of 97.25%. However, due to the high number of parameters involved in the transfer learning approach, the model experienced significant computational complexity.

In 2020, Hameed et al. investigated deep learning models for breast cancer classification in their publication "Ensembles of Deep Learning Models" [9]. They employed pre-trained VGG-16 and VGG-19 architectures, as well as a 544-image custom dataset. This dataset was divided into training and testing sets with an 80:20 ratio. The classification accuracy of VGG-16 and VGG-19 was 91.67% and 90.35%, respectively. Combining VGG-16 and VGG-19 in a fine-tuned model resulted in a classification accuracy of 95.29% for discriminating between benign and malignant tumors.

Using a variety of machine learning methods, such as K-Nearest Neighbor, Logistic Regression, Decision Tree, Random Forest, Support Vector Machine, and Deep Learning Artificial Neural Network (DLANN), Gupta et al. suggested a breast cancer prediction model in their 2020 study [10]. They made use of the 569-image Wisconsin Breast Cancer Dataset (WDBC). K-Nearest Neighbor, Logistic Regression, and Decision Tree reported accuracies of 95.8%; Random Forest and Support Vector Machine recorded 97.2%; while the DLANN technique yielded the best accuracy of 97.24%.

Zhenget et al. [11] released their paper, Deep learning assisted efficient adaboost algorithm for breast cancer detection and early diagnosis, in 2020. They used the Cancer Imaging Archive Dataset (TCIA) to construct a Deep Learning-Assisted Efficient Ada-boost Algorithm (DLAEABA). This model calculated an average accuracy rating of 97.2%.

In 2020, Krithiga et al. published a work titled Deep learning-based breast cancer detection and classification with fuzzy merging algorithms [12]. This paper used many machine learning methods such as Support Vector Machine, Random Forest, VGG-16, and custom CNN. Author used The Cancer Image Archive (TCIA) and a custom collected Dataset to differentiate a tumor between Benign and Malignant. The Dataset consists of 9109 total ultrasound images which then is processed through VGG-16, AlexNet, GoogLeNet and SGNet and has achieved accuracy of 91.8%, 93.8%, 95.8%, 96.6% respectively. The author also implemented a custom CNN and has got the highest accuracy of 96.62%.

Authors Yesim et al. suggested a hybrid approach based on Convolutional Neural Net-works for classifying breast ultrasonography pictures as benign, malignant, and normal using mRMR in 2021 [13]. Author used Hybrid based CNN including AlexNet, Mo-bilenetv2 and Res-Net50 as a base for hybrid structure. Author has used a Europe PMC dataset which consisted 780 images of benign, malignant and normal images. Author has gained 95.6% prediction accuracy using proposed hybrid model + SVM model.

In 2023, M.K. Laksath et al. suggested a Multibranch Unet-Based Segmentation and Classification-Based Diagnosis of Tumors From Breast Ultrasound Images [14]. Au-thor used Breast Ultrasound Images Dataset that consisted total image of size 780. Author increased data set size by augmentation technique. Training and Testing dataset was done with the split ratio of 70:30 respectively. Author got the prediction accuracy of 76%.

In 2020, Nrea et. al proposed a Breast Cancer Detection using Convolution Networks [15]. Author implemented a Custom CNN model using a custom collected X-Ray Image Dataset in which 1588 full mammogram images including mass abnormalities. Author divided dataset into 80% for training, 10% for validation and remaining 10% for testing purpose respectively. Five-layer CNN model results in detection accuracy of 91.86%.

Transfer learning is the process of converting a deep learning model (such as Inception V3) that has previously learnt from a vast quantity of data, usually a general dataset like ImageNet, to a specific objective, such as categorizing breast cancer photos. In-stead of beginning from zero, transfer learning enables us to use the model's existing knowledge and features, saving time and computational resources.

In their paper "Breast Cancer Detection and Classification Empowered With Transfer Learning," the authors of [16] proposed a transfer learning model for classifying breast cancer tumors as benign, malignant, or normal. Results verified with cross validations, heatmaps, confusion matrix for ultra sound images of all three categories, authors compared the results with other variants of transfer learning approach like AlexNet, VGG-16, Inception, ResNet and NasNet. Proposed Modified Alexnet approach outperformed other approaches in terms of accuracy with 96.4% for dataset "A," 96.7% with dataset B.

The authors in [17] implemented three different CNNs to detect breast cancer from mammograms. Author suggests to use transfer learning for breast cancer detection be-cause having insufficient numbers of limited mammographic images in not feasible to train CNN from scratch. They utilize transfer learning to make use of existing pre-trained models. The proposed model is created by integrating pretrained VGG-16 with 1-FC NN-classifier. These models are capable of categorizing breast cancer into three groups Benign, Malignant, or Normal with the accuracy of 90.5%.

TABLE I.   COMPARATIVE STUDY OF CLASSIFICATION OF BREAST CANCER   IMAGES USING CNN AND TRANSFER LEARNING

Reference	Year of publishing	Data Set	Total images	Algorithm	Accuracy
[8]	2019	Standard Benchmark Dataset and Locally Developed Dataset	8000	Custom CNN	97.25%
				GoogleNet	93.5%
				VGGNet	94.15%
				ResNet	94.35%
[9]	2020	Custom Dataset Collection	544	Fine Tuned VGG-16+VGG-19	95.29%
				VGG-16	91.67%
				VGG-19	90.35%
[10]	2020	WDBC	569	Deep learning using ANN	97.24%
				KNN	95.8%
				SVM	97.2%
				LR	95.8%
				DT	95.8%
				RF	97.2%
[11]	2020	TCIA	-	DLAEABA	97.2%
[12]	2020	TCIA	9109	Custom CNN	96.62%
				VGG-16	91.8%
				AlexNet	93.8%
				GoogleNet	95.8%
				SgNet	96.6%
[13]	2021	Europe PMC	780	Custom hybrid model + SVM	95.6%
[14]	2023	Breast Ultrasound Image Dataset	780	Custom CNN	76%
[15]	2021	Custom Dataset Collection	1588	Custom CNN	90.5%

In 2020, M. Byra et al. conducted research on the segmentation of breast mass in ultra-sonography using a selective kernel U-Net convolutional neural network [18]. Author has used three different datasets namely UDIAT, OASBUD and BUSI with 163, 100 and 697 images having Benign and Malignant breast health condition respectively. Each dataset was randomly divided into Training and Testing set comprising of 50% for training and remaining 50% for testing. Image size used in this research was 224x224 pixels after pre-processing. Author concluded that proposed SK-UNet model outperformed regular U-Net model in Mean Dice score of 0.826, Accuracy of 0.979, AUC with 0.958 and Detection rate of 0.900.

In year 2020, author P.Vianna et. al proposed U-Net and SegNet performances on lesion segmentation of breast ultrasonography images [19]. Author has collected a dataset from National Cancer Institute of Rio de Janeiro, Brazil with the total number of 2054 images of which Benign with 1351 and Malignant with 703. The size of the im-age used for this study was 128x128 after pre-processing and Training, Validation and Testing split ratio used was 70:10:20 respectively. Author concluded that U-Net model performed better than SegNet with dice coefficient of 86.3% and dice score of 81.1%.

Liu et.al on 2024 performed research on An asymmetric U-shape network for lesion segmentation of breast cancer and named as AsymUnet. Author has used 2 different datasets one with BUSI dataset that has 645 total number of Benign and Malignant im-ages with 70:15:15 for Train, Test and Validation ratio and another dataset termed as Dataset B collected by Yap et.al [20] with 163 lesion images with 60:20:20 for Train, Test and Validation split ratio. Both datasets were resized into 256x256 pixels after pre-processing. On BUSI dataset, author achieved scores of 71.34%, 79.94%, and 78.11% on the Jaccard, Dice, and Recall metrics, respectively. However, on Dataset B, Jaccard, Dice, Accuracy, Recall, and Precision indicators reached 75.56%, 83.25%, 98.15%, 78.90%, and 93.18%, respectively.

Ronneberger et al. (2015) introduces a UNet strategy for segmentation of microscopy images using data augmentation [21]. The architecture consists of a U-shaped contracting path and an expanding path. The paper claims superior performance compared to previous convolutional for a particular set of microscopic images. Experimental validation was conducted on a training dataset sourced from the ISBI 2012 challenge. The Unet demonstrates particularly fast segmentation when equipped with a Graphical Processing Unit. Unfortunately, the Ronneberger's strategy has been applied to a rela-tively small dataset.

Khaledyan et al. (2023) presents pre-processing, combination of various optimization techniques, and fine-tuning of different variants of UNet for the breast US images [22]. UNet, Sharp UNet(Zunair and Hamza, 2021) and Attention UNet (Oktay et al., 1804) are combined. Building upon these variants, a novel Sharp Attention UNet is proposed. The specificity, Dice coefficient, F10score, and sensitivity are reported as 0.99, 0.93, 0.94, and 0.94 respectively. McNemar's statistical test indicates that the proposed Sharp Attention UNet outperforms all other models tested against the conventional Unet.

TABLE II.   COMPARATIVE ANALYSIS WITH STATE-OF-ARTS METHODS

Ref	Year of publishing	Data Set	Image Category	Total images	Image Size	Algorithm	Dice Score
[18]	2020	UDIAT: 163 OASBUD: 100 BUSI: 697	Benign and Malignant	882	224x224	U-Net Sk-UNet	82.6% by Sk-UNet
[19]	2020	Custom Collected	Benign and Malignant	2054	128x128	U-Net SegNet	81.1% by U-Net
[20]	2024	BUSI= 645 Yap et.al Dataset B= 163	Benign and Malignant only	808	256x256	Asym-Unet (Custom)	79.94% on BUSI Dataset, 83.25% on Dataset B
[21]	2015	ISBI 2012 EM segmentation challenge. Training = 30	neuronal cells and their membranes. (electron microscopy (EM) images)	30	512x512	UNet architecture	No dice score used instead used Warping Error: 0.0003529 Rand Error: 0.0382
[22]	2023	(BUSI) dataset. Normal= 133 Benign = 210 Malignant = 437	normal, benign, and malignant	780	600 x 500	Sharp Attention UNet	93%
[23]	2022	Custom collected from Sun Yat-Sen University Training = 910 Testing = 207	Benign (images of the median nerve without any disease conditions)	1117	—	VGG16-UNet enhanced with attention mechanisms and residual modules	0.904 ± 0.035

Huang et al. (2022) enhance the accuracy of segmentation of the median nerve in the arm and forearm in US images using the DL [23]. An improved network, VGG16-UNet, has been proposed, combining the VGG16 model and the UNet. The model is further augmented with attention mechanisms and residual modules. Trained on a dataset of 910 images and

tested on 207 frames, the model was by the region-based metrics above. The results indicate a significant improvement (statistically p < 0.01) regarding AS-UNet ranking the highest. The VGG16-UNet shows Jaccard = 0.826±0.057, Recall = 0.909±0.061, Dice = 0.904±0.035, and Precision = 0.905±0.061.

Comparative analysis for the segmentation of breast cancer is shown in table 2.2 on to conclude the research gap. Year of publishing, dataset used, Image category, total no. of images, image size, algorithm used and obtained dice score used is compared.

III. RESEARCH METHODOLOGY

The system model in Figure 8 explains the overall implementation model of the study. Ultrasound classification dataset [24] fed as data with the necessary initialization.
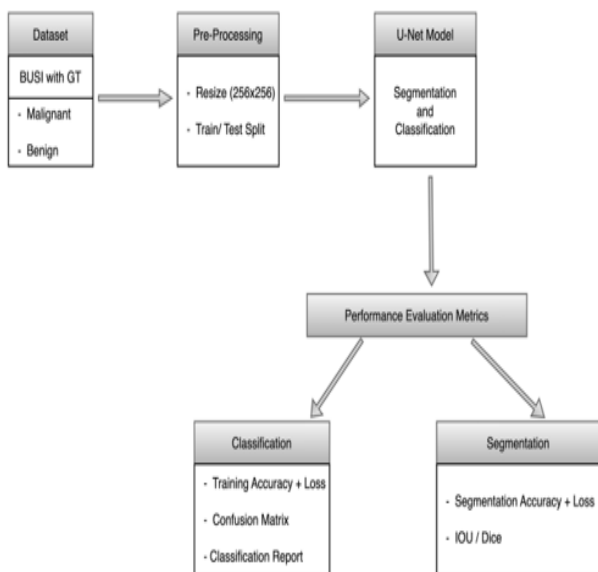

Fig. 8. Methodology

1) Data Collection

Breast ultrasound pictures from women between the ages of 25 and 75 that were gathered in 2018 are included in the baseline data [25]. A total of 780 photos with a resolution of approx. 500x500 pixels are included in the collection, which includes photographs from 600 female patients. Every picture is in PNG format. Alongside the original pictures there are ground truth pictures too. Three categories—normal, benign, and malignant—are applied to the photographs. However, the benign and malignant classifications are the only focus of this investigation.

TABLE III.   IMAGE COUNT ON INDIVIDUAL CATEGORY

Dataset-BUSI-with-GT	
Benign Condition	437
Malignant Condition	210
Normal Condition	133
Total:	780

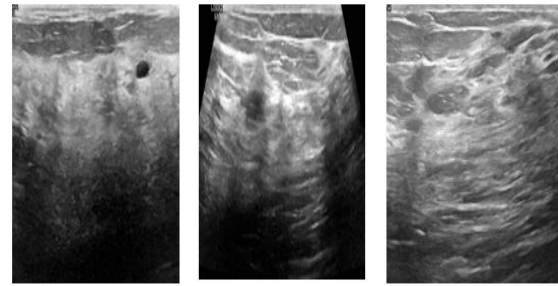Fig(a) Benign   Fig(b) Malignant   Fig(c) Normal

Fig. 9. Sample images from BUSI-with-GT dataset

2) Pre-processing

Dataset contained a variable sized images which are further resized into a 256x256 pixels size suitable for the proposed model. Two different labels are defined. For classification, Grayscale with image categories as ['benign', 'malignant'] are defined. For segmentation, grayscale images along with their ground truth are define. Both the data format is passed to the model.

After resizing the images for breast cancer segmentation using U-Net, we proceeded to split the dataset into (80:10:10) for Train, Test and Validation sets where 80% of the total dataset distributed for training, for validation set 10% and remaining 10% for testing. This split ensures that the model learns from a different range of examples during training phase and then calculated its performance on unseen data during testing phase.

3) U-Net Architecture

The encoder and decoder portions of the U-Net architecture are connected by skip links between appropriate layers. During training, the vanishing gradient issue is lessened and spatial information is retained because to these skip connections.
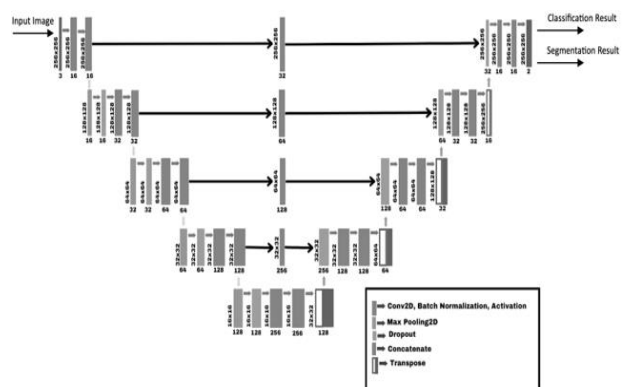

Fig. 10. U-Net Architecture

The U-Net Architecture consist of following layers

- Convolutional Block Layers

   Conv2D: Applies a 3x3 convolution with a specified number of filters, ensuring feature extraction.

Batch Normalization: Normalizes the output of the convolution for stable training.

Activation (ReLU): Introduces non-linearity to the network, aiding in feature learning.

Dropout: Randomly drops a specified fraction of neurons, preventing overfitting.

- Residual Block Layers

Convolutional Blocks: Two consecutive convolutional blocks for feature extraction.

Conv2D (1x1 kernel for skip connection): 1x1 convolution to match dimensions for the skip connection.

Dropout: Introduces regularization to the residual block.

Add (for skip connection): Combines the output of the convolutional blocks with the residual connection.

- Encoder Block Layers

Convolutional Blocks: Three convolutional blocks for feature extraction.

MaxPooling2D: Down samples the spatial dimensions by selecting the maximum value in each region.

- Decoder Block Layers

Conv2DTranspose (Transpose Convolution): Up samples the input to match the skip connection's spatial dimensions.

Dropout: Introduces regularization to the decoder block.

Concatenate (for skip connection): Concatenates the upsampled features with the skip connection from the encoder.

Convolutional Blocks: Three consecutive convolutional blocks for feature extraction.

- Dual Output Branches

The model branches into two outputs after the final convolutional block

- Classification Branch

Flatten: The output of the last convolutional block is flattened.

Dense Layer: A dense layer with 64 units and ReLU activation.

Output Layer: A dense layer with a single unit and sigmoid activation, named classification_output. This layer provides a binary classification_output.

- Segmentation Branch

Conv2D Layer: A convolutional layer with 1 filter, kernel size (1, 1) and sigmoid activation, named segmentation output. This layer provides a segmentation map output.

This U-Net model is designed to perform both classification and segmentation simultaneously. The encoder path captures features and context, while the decoder path refines these features and restores spatial resolution. The dual-output design allows the model to produce a binary classification (e.g., presence or absence of a certain feature) and a segmentation map (e.g., pixel-wise classification) in a single forward pass. This architecture is particularly useful in medical imaging, where identifying both the presence of anomalies and their precise locations is crucial.

The U-Net model is set up for training by the model.compile line, which also sets the optimizer, metrics, and loss functions. It makes use of the Adam optimizer, which is renowned for its effectiveness in dynamically modifying learning rates during deep learning model training. Both outputs have defined loss functions: binary cross-entropy for managing binary segmentation pixel-by-pixel in the segmentation_output and binary cross-entropy for handling binary classification tasks in the classification_output. Furthermore, the statistic 'accuracy', which quantifies the percentage of accurate predictions, is set for both outputs. This configuration guarantees that the model is suitably tuned and assessed for tasks involving both segmentation and classification.

4) Activation functions

In neural networks, the Rectified Linear Unit (ReLU) is a popular activation function.

$$f(x) = \max(0,x) \tag{1}$$

Equation defines it, with x serving as the function's input. ReLu is a piecewise line-ar function that yields 0 in the absence of a positive input and returns the input if it is. Because of its simplicity and ability to prevent the vanishing gradient problem, it has become the chosen activation function in several applications involving deep learning. ReLu is also more computationally efficient and easy to optimize.

B. Performance Evaluation Metrics (PEM)

1) PEM of Classification

One approach for evaluating a classification model's efficacy is a confusion matrix. It shows the counts of false positives, false negatives, true positives and true negatives counts that are necessary for computing performance metrics like as recall, accuracy, precision, and F1 score. Table 4 presents the classification model's con-fusion matrix. The confusion matrix uses the following core terminologies:

TABLE IV.   CONFUSION MATRIX

		Actual	
		Positive	Negative
Predicted	Positive	True Positive	False Positive
	Negative	False Negative	True Negative

True Positives (TP): This is the number of examples that the model correctly recognizes as being in the positive class.

True Negatives (TN): This is the amount of cases where the predicted class and the actual class are both negative.

False Positives (FP): In some cases, the model predicts the presence of a condition when it is actually lacking, wrongly classifying a negative event as positive.

False Negatives (FN): This is the number of cases where the model predicts a negative outcome when, in fact, the data is positive.

Statistical metrics such as accuracy, F-score, precision, and recall are used to evaluate a classification model's performance. True positives, true negatives, false positives, and false negatives are represented here by the letters TP, TN, FP, and FN, in that order.

Precision: The percentage of accurately detected positive occurrences among all instances projected to be positive is used as a metric to assess the effectiveness of the classification model. It is calculated by dividing the total number of false positives and true positives by the number of true positives.

$$Precision(P) = \frac{T_P}{T_P + F_P} \tag{2}$$

Recall: Recall is a performance indicator that evaluates the percentage of real positive cases that the classification model properly identifies. It is also known as sensitivity or the true positive rate. It is computed as the ratio of true positives to the total of true positives and false negatives, and it indicates the model's capacity to identify positive cases.

$$Recall(R) = \frac{T_P}{T_P + F_N} \tag{3}$$

F1-score: By integrating precision and recall into a single number, the F1 score is a statistic used to assess the correctness of a model. It is the harmonic mean of recall, which measures the proportion of real positives to all actual positives, and precision, which measures the ratio of genuine positives to all anticipated positives. Higher numbers on the F1 score scale, which goes from 0 to 1, denote superior performance. Because it offers a more comprehensive picture of the model's performance than accuracy alone, this statistic is especially helpful for evaluating models with unbalanced class distributions.

$$F1 - score = 2 \times \frac{P \times R}{P + R} \tag{4}$$

Accuracy: The Accuracy is a performance indicator that shows the percentage of examples in the dataset that are correctly classified in relation to the total number of instances in the dataset. The calculation involves dividing the total number of instances by the sum of true positives and true negatives. A classification model's overall effectiveness can be broadly evaluated using accuracy.

$$Accuracy(A) = \frac{T_P + T_N}{T_P + T_N + F_P + F_N} \tag{5}$$

2) PEM of Segmentation
The following are the definitions of true positive, false positive, true negative, and false negative in the context of picture segmentation:

True Positives: Pixels identified as 1 in both the ground truth and the expected mask are referred to as True Positives (TP).

False Positives: Pixels that have a ground truth of 0 but a predicted mask label of 1 are known as False Positives (FP).

False Negatives: Pixels that have a ground truth of 1 but a predicted mask label of 0 are known as False Negatives (FN).

True Negatives: Pixels identified as 0 in both the ground truth and the expected mask are known as True Negatives (TN).

Dice coefficient : The Dice coefficient is a metric used to measure how similar two sets are. It is particularly useful for evaluating the correspondence between predicted and actual segmentation masks. The Dice coefficient ranges from 0 to 1, where a value of 1 signifies complete alignment between the predicted and true segmentations, while a value of 0 indicates no overlap between them.

$$Dice = \frac{2 \times Intersection + 1}{Total\ pixels\ in\ y_{true} + Total\ pixels\ in\ y_{pred}} \tag{6}$$

Where:

ytrue is the ground truth segmentation mask

ypred is the predicted segmentation mask

Intersection is the sum of element wise multiplication of ytrue and ypred

Total pixels in ytrue is the sum of all pixels in the ground truth mask

Total pixels in ypred is the sum of all pixels in the predicted mask

IoU: The Jaccard Index, or Intersection over Union (IoU) statistic, measures the amount of spatial overlap between segmentation masks that are predicted and those that are based on ground truth. Tasks involving picture segmentation frequently make use of it.

$$IoU = \frac{Intersection + 1}{Union + 1} \tag{6}$$

Where,

Intersection is the total of the element-by-element multiplication of the flattened true and anticipated masks is the intersection.

Union is the sum of true and predicted masks minus the intersection

The addition of 1 in the numerator and denominator is a smoothing factor to handle cases where both masks are empty, preventing division by zero

F1-Score: A statistic called the F1 Score provides a single value for assessing the effective-ness of a binary classification model by striking a balance between precision and recall. The Eq.4 shows the equation of F1-score.

IoU Loss : The IoU Loss is a custom loss function designed to be minimized during the training of segmentation

models. It is based on the IoU metric. Intersection and Union are defined as in the IoU metric, and Smooth is a smoothing factor to prevent division by zero.

$$IoU\ Loss = 1 - IoU \tag{9}$$

Where

$$IoU = \frac{Intersection + Smooth}{Union + Smooth} \tag{10}$$

C. Motivation Behind Algorithm Selection

The motivation behind the U-Net mode, designed to provide both classification and segmentation outputs, is driven by the need to address complex tasks in image processing, particularly in fields like medical imaging [26].

1) Dual Task Compatibility

The model can simultaneously perform classification (e.g., detecting the presence of a disease) and segmentation (e.g., identifying the precise location and boundaries of affected areas). This dual capability is efficient and can save computational resources and time compared to training separate models for each task.

2) Efficiency and Resource Utilization

The model can efficiently learn and reuse features that are relevant for both classification and segmentation. This reduces the total number of parameters and computational load compared to having separate models.
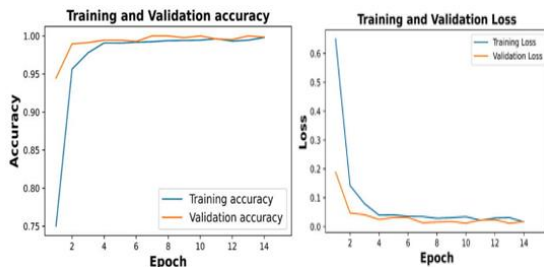

Fig. 11. Training and Validation Accuracy and Loss

3) Enhance Learning Through Joint Training

Joint training of classification and segmentation tasks can act as a regularizer, potentially improving the generalization of the model. The shared layers learn features that are useful for both tasks, leading to more robust feature representations.

IV. RESULT AND DISCUSSION

A. Environment Setup and Tools Used

Python was used in the development of the U-Net model, and Google Colab was used for experimentation. To speed up processing, this cloud-based platform made use of an NVIDIA K80 GPU with RAM consisting of 12 GB, which was offered by Google. Versions 3.7 of Python, 2.5.0 of Keras, and 2.5.0 of the TensorFlow framework were setup in the Google Colab runtime environment to guarantee a stable configuration for model training and evaluation.

1) Tools Used

Python is the preferred choice for U-Net for multiclass breast cancer classification" due to its rich libraries like TensorFlow and Keras, simplicity, strong community support, and compatibility with tools like Jupyter Notebooks. Its versatility allows for quick prototyping and seamless integration with data manipulation and visualization libraries, enabling efficient development of U-Net based models for this task.

Jupyter Notebook is popular in research for its interactive and flexible nature, allowing researchers to combine code, visualizations, and explanatory text in a single document. It facilitates reproducibility, collaboration, and sharing of findings, making it an effective tool for analyzing data, conducting experiments, and presenting results in an accessible manner.

B. Result Analysis

1) Classification Result

Standard statistical validation methods were employed, including the assessment of accuracy and loss of the proposed model against training image set, test set, and vali-dation sets. Furthermore, measures such as accuracy, F1-score, and recall were employed to assess the model's effectiveness.

Every training fold was set up to use early stopping through callbacks that tracked the validation loss for a total of 15 epochs. If the validation loss did not improve after three epochs, training would end. The model was trained for ten folds, and Figure 11 displays the accuracy and loss graphs at the end of the training process.

The model attained an average training accuracy of 98.36 ± 0.62%, a validation ac-curacy of 98.30 ± 0.94% and an average test accuracy of 99.08 ± 0.64% across the 10-fold cross-validation (as detailed in Table 5)

TABLE V. K=10 FOLD VALIDATION RESULT

	TA	TL	VA	VL	TsA	TsL
K1	98.9000	0.0036	99.0000	0.0001	98.0000	0.04
K2	96.9900	0.6236	97.4500	0.2445	99.0000	0.01
K3	98.9000	0.0008	99.0000	0.0000	98.0000	0.09
K4	98.6100	0.0082	99.0000	0.0036	96.6700	0.04
K5	98.3200	0.9420	99.0000	0.0000	98.2200	0.03
K6	97.8400	0.1851	96.6700	0.3579	98.1100	0.62
K7	97.7400	0.1261	98.2200	0.0632	98.2200	0.07
K8	98.6100	0.0122	99.0000	0.0014	98.2200	0.01
K9	98.7100	0.0254	96.6700	0.2454	97.4500	0.30
K10	99.0000	0.0037	99.0000	0.0039	99.0000	0.01
μ ± σ	98.36±0.62	0.19±0.31	98.30±0.94	0.092±0.13	98.08±0.64	0.122±0.18

The model demonstrates strong performance in detecting both malignant and benign categories. For malignant cases, it achieves an average specificity of 98.41%, sensitivity of 99.93%, precision of 99.23%, F-score of 99.18%, and recall of 97.77%. For benign cases, the model shows an average specificity of 99.93%, sensitivity of 98.41%, precision of 98.17%, F-score of 98.83%, and recall of 99.53%. This indicates a high accuracy and reliability in classifying both types of breast lesions, with slightly better precision and recall for benign cases.

TABLE VI.   SENSITIVITY, SPECIFICITY, PRECISION, RECALL AND
F1-SCORE

		Spec	Sen	Pre	Fsc	Rec
K1	Malignant	99.34	100.00	98.31	99.98	99.15
	Benign	100.00	99.34	98.56	98.78	99.56
K2	Malignant	97.26	100.00	96.55	98.25	100.00
	Benign	100.00	97.26	100.00	98.61	97.26
K3	Malignant	100.00	100.00	100.00	99.12	99.34
	Benign	100.00	100.00	99.54	98.67	99.76
K4	Malignant	99.50	100.00	98.12	99.34	99.89
	Benign	100.00	99.50	98.90	99.38	98.86
K5	Malignant	100.00	100.00	100.00	100.00	100.00
	Benign	100.00	100.00	100.00	100.00	100.00
K6	Malignant	96.25	100.00	100.00	98.09	96.25
	Benign	100.00	96.25	94.23	97.03	100.00
K7	Malignant	96.10	99.25	100.00	99.20	97.34
	Benign	99.25	96.10	95.32	98.30	99.89
K8	Malignant	100.00	100.00	100.00	100.00	100.00
	Benign	100.00	100.00	100.00	100.00	100.00
K9	Malignant	95.71	100.00	100.00	97.81	95.71
	Benign	100.00	95.71	95.16	97.52	100
K10	Malignant	100.00	100.00	100.00	100.00	100.00
	Benign	100.00	100.00	100.00	100.00	100.00
$\mu \pm \sigma$	Malignant	98.41 ± 1.75	99.93 ± 0.23	99.23 ± 1.15	99.18 ± 0.81	98.77 ± 1.59
	Benign	99.93 ± 0.23	98.41 ± 1.75	98.17 ± 2.20	98.83 ± 0.98	99.53 ± 0.83

10% of benign and malignant data from the dataset was used to test model. For actual malignant cases, the model correctly identified 32 instances but misclassified 1 as benign. For actual benign cases, the model accurately predicted 29 instances and mis-classified 2 as malignant. This indicates the model has high accuracy, with very few misclassifications, effectively distinguishing between malignant and benign cases.

TABLE VII.   CONFUSION MATRIX FOR TEST DATA

		Predicted	
		Malignant	Benign
Actual	Malignant	32	1
	Benign	2	29

C. Segmentation Result for Test Result

The original image for grayscale, ground truth and predicted mask is shown in Table 8. The image selection is random where some simple (For Example VI) and some complex images (For example II and IV) are considered'.

D. Statistical Comparison with other state of arts methods

Table 10 compares various segmentation models based on their performance metrics. The models achieve high accuracies (up to 98.5%) and specificities (above 99%), with notable variations in precision, F1 Score, Dice coefficient, and IoU. The "Proposed" model stands out with the highest precision (0.954) and IoU (0.890) among the listed architectures.

TABLE VIII.   PREDICTED MASK FOR TEST DATA

TABLE IX.   TABLE 9: STATISTICAL RESULT

Image	Accuracy	Precision	Specificity	F1 Score	Recall	IoU
I	0.99542	0.97591	0.99875	0.94350	0.96589	0.89335
II	0.99613	0.97215	0.99855	0.94608	0.97254	0.89790
III	0.99583	0.97878	0.99846	0.95537	0.97488	0.91493
IV	0.99555	0.97894	0.99806	0.95760	0.97670	0.91901
V	0.99675	0.95836	0.99802	0.93033	0.97046	0.86973
VI	0.99618	0.97834	0.99887	0.95289	0.97316	0.91044

TABLE X.   TATISTICAL COMPARISON WITH OTHER STATE OF ARTS METHODS

Model	Accuracy	Precision	F1 Score	Specificity	DICE	IoU
UNet (Ronneberger et al., 2015) [21]	0.982	0.911	0.867	0.994	0.861	0.756
Attention UNet (Oktay et al., 2018) [27]	0.984	0.924	0.899	0.994	0.894	0.808
Sharp UNet (Zunair and Hamza, 2021) [28]	0.984	0.885	0.886	0.992	0.877	0.781
UNet++ (Zhou et al., 2018) [29]	0.978	0.864	0.854	0.987	0.847	0.772
UNet3++ (Huang et al., 2020) [23]	0.981	0.896	0.875	0.992	0.865	0.775
Sharp Attention UNet (Khaledyan et al., 2023) [30]	0.979	0.941	0.942	0.994	0.928	0.866
Proposed	0.985	0.954	0.947	0.992	0.947	0.890

V. CONCLUSION

The study utilized two distinct types of input data: grayscale ultrasound images with labels for classification and grayscale images with ground truth masks for segmentation. The model was trained with an 80% of dataset for training, with 10% for Testing set and remaining 10% for validation set. The proposed model achieved a training accuracy of $98.36 \pm 0.62\%$, validation accuracy of $98.30 \pm 0.94\%$, and testing accuracy of $98.08 \pm 0.64\%$ for classification. The corresponding training, validation, and testing losses were 0.19 ± 0.31, 0.092 ± 0.13, and 0.122 ± 0.18, respectively. For segmentation, the model achieved an Intersection over Union (IoU) value of 89.089%.

These promising results underscore the potential of the multi-tasking UNet architecture in advancing medical image analysis, thereby contributing to improved diagnostic and treatment strategies for breast cancer patients. Future enhancements to this study could involve integrating more diverse datasets to further validate the model's robustness and generalizability across different imaging modalities and patient demographics. Additionally, incorporating advanced techniques like attention mechanisms and transfer learning could enhance the model's performance and efficiency.

REFERENCES

[1] "Breast Cancer," World Health Organization, Jun. 2021. [Online]. Available: http://www.who.int/news-room/fact-sheets/detail/breast-cancer.

[2] H. Sung et al., "Global Cancer Statistics 2020: GLOBOCAN Estimates of Incidence and Mortality Worldwide for 36 Cancers in 185 Countries," CA: a Cancer Journal for Clini-cians, vol. 71, no. 3, pp. 209–249, Feb. 2021, doi: https://doi.org/10.3322/caac.21660.

[3] "Nepal Source: GLOBOCAN 2020." Available: https://gco.iarc.fr/today/data/factsheets/populations/524-nepal-fact-sheets.pdf

[4] N. Siddique, S. Paheding, C. P. Elkin, and V. Devabhaktuni, "U-Net and Its Variants for Medical Image Segmentation: A Review of Theory and Applications," IEEE Access, vol. 9, pp. 82031–82057, 2021, doi: https://doi.org/10.1109/access.2021.3086020.

[5] O. Ronneberger, P. Fischer, and T. Brox, "U-net: Convolutional networks for biomedical image segmentation," 2015, pp. 234–241.

[6] J. Long, E. Shelhamer, and T. Darrell, "Fully convolutional networks for semantic seg-mentation," 2015, pp. 3431–3440.

[7] "National Breast Cancer Foundation," National Breast Cancer Foundation, 2019. https://www.nationalbreastcancer.org/breast-tumors/

[8] S. Khan, N. Islam, Z. Jan, I. Ud Din, and J. J. P. C. Rodrigues, "A novel deep learning based framework for the detection and classification of breast cancer using transfer learn-ing," Pattern Recognition Letters, vol. 125, pp. 1–6, Jul. 2019, doi: https://doi.org/10.1016/j.patrec.2019.03.022.

[9] Z. Hameed, S. Zahia, B. Garcia-Zapirain, J. Javier Aguirre, and A. María Vanegas, "Breast Cancer Histopathology Image Classification Using an Ensemble of Deep Learning Mod-els," Sensors, vol. 20, no. 16, p. 4373, Aug. 2020, doi: https://doi.org/10.3390/s20164373.

[10] P. Gupta and S. Garg, "Breast Cancer Prediction using varying Parameters of Machine Learning Models," Procedia Computer Science, vol. 171, pp. 593–601, 2020, doi: https://doi.org/10.1016/j.procs.2020.04.064.

[11] J. Zheng, D. Lin, Z. Gao, S. Wang, M. He, and J. Fan, "Deep Learning Assisted Efficient AdaBoost Algorithm for Breast Cancer Detection and Early Diagnosis," IEEE Access, vol. 8, pp. 96946–96954, 2020, doi: https://doi.org/10.1109/ACCESS.2020.2993536.

[12] R. Krithiga and P. Geetha, "Deep learning based breast cancer detection and classification using fuzzy merging techniques," Machine Vision and Applications, vol. 31, no. 7–8, Sep. 2020, doi: https://doi.org/10.1007/s00138-020-01122-0.

[13] Y. Eroğlu, M. Yildirim, and A. Çinar, "Convolutional Neural Networks based classification of breast ultrasonography images by hybrid method with respect to benign, malignant, and normal using mRMR," Computers in Biology and Medicine, vol. 133, p. 104407, Jun. 2021, doi: https://doi.org/10.1016/j.compbiomed.2021.104407.

[14] M. K. Laksath Adityan, H. Sharma and A. Paul, "Segmentation and Classification-Based Diagnosis of Tumors From Breast Ultrasound Images Using Multibranch Unet," 2023 IEEE International Conference on Image Processing (ICIP), Kuala Lumpur, Malaysia, 2023, pp. 2505-2509, doi: 10.1109/ICIP49359.2023.10222147.

[15] Nrea et.al, Breast Cancer Detection Using Convolutional Neural Networks. AI4AH ICLR, 2020 (2020), pp. 1-8

[16] S. Arooj et al., "Breast Cancer Detection and Classification Empowered With Transfer Learning," Frontiers in Public Health, vol. 10, Jul. 2022, doi: https://doi.org/10.3389/fpubh.2022.924432.

[17] S. Guan and M. Loew, "Breast Cancer Detection Using Transfer Learning in Convolutional Neural Networks," IEEE Xplore, Oct. 01, 2017. https://ieeexplore.ieee.org/abstract/document/8457948.

[18] M. Byra et al., "Breast mass segmentation in ultrasound with selective kernel U-Net con-volutional neural network," Biomedical Signal Processing and Control, vol. 61, p. 102027, Aug. 2020, doi: https://doi.org/10.1016/j.bspc.2020.102027.

[19] P. Vianna, R. Farias, and W. C. de Albuquerque Pereira, "U-Net and SegNet performances on lesion segmentation of breast ultrasonography images," Research on Biomedical Engi-neering, Mar. 2021, doi: https://doi.org/10.1007/s42600-021-00137-4.

[20] J. Liu et al., "Asym-Unet: An Asymmetric U-Shape Network for Lesion Segmentation of Breast Cancer," Jan. 2024, doi: https://doi.org/10.2139/ssrn.4676212.

[21] O. Ronneberger, P. Fischer, and T. Brox, "U-Net: Convolutional networks for biomedical image segmentation," arXiv (Cornell University), May 2015, doi: https://doi.org/10.48550/arxiv.1505.04597.

[22] D. Khaledyan, T. J. Marini, T. M. Baran, Avice O'Connell, and K. Parker, "Enhancing breast ultrasound segmentation through fine-tuning and optimization techniques: Sharp at-tention UNet," PloS one, vol. 18, no. 12, pp. e0289195–e0289195, Dec. 2023, doi: https://doi.org/10.1371/journal.pone.0289195.

[23] A. Huang, L. Jiang, J. Zhang, and Q. Wang, "Attention-VGG16-UNet: a novel deep learn-ing approach for automatic segmentation of the median nerve in ultrasound imag-es," Quantitative imaging in medicine and surgery, vol. 12, no. 6, pp. 3138–3150, Jun. 2022, doi: https://doi.org/10.21037/qims-21-1074.

[24] "Dataset-BUSI-with-GT"www.kaggle.com. https://www.kaggle.com/datasets/anaselmasry/datasetbusiwithgt

[25] Al-Dhabyani W, Gomaa M, Khaled H, Fahmy A. Dataset of breast ultrasound images. Da-ta in Brief. 2020 Feb;28:104863. DOI: 10.1016/j.dib.2019.104863

[26] G. Du, X. Cao, J. Liang, X. Chen, and Y. Zhan, "Medical Image Segmentation based on U-Net: A Review," Journal of Imaging Science and Technology, vol. 64, no. 2, pp. 20508–20508, Mar. 2020, doi: https://doi.org/10.2352/j.imagingsci.technol.2020.64.2.020508.

[27] Oktay, O., Schlemper, J., Folgoc, L.L., Lee, M., Heinrich, M., Misawa, K., Mori, K., McDonagh, S., Hammerla, N.Y., Kainz, B., et al., 1804. Attention u-net: Learning where to look for the pancreas. arxiv 2018. arXiv preprint arXiv:1804.03999.

[28] Zunair, H., Hamza, A.B., 2021. Sharp u-net: Depthwise convolutional network for biomed-ical image segmentation. Computers in biology and medicine 136, 104699.

[29] Zhou, Z., Rahman Siddiquee, M.M., Tajbakhsh, N., Liang, J., 2018. Unet++: A nested u-net architecture for medical image segmentation, in: Deep Learning in Medical Image Analysis and Multimodal Learning for Clinical Decision Support: 4th International Work-shop, DLMIA 2018, and 8th International Workshop, ML-CDS 2018, Held in Conjunction with MICCAI 2018, Granada, Spain, September 20, 2018, Proceedings 4, Springer. pp. 3–11.

[30] Khaledyan, D., Marini, T.J., M. Baran, T., O'Connell, A., Parker, K., 2023. Enhancing breast ultrasound segmentation through fine-tuning and optimization techniques: Sharp at-tention unet. Plos one 18, e0289195.